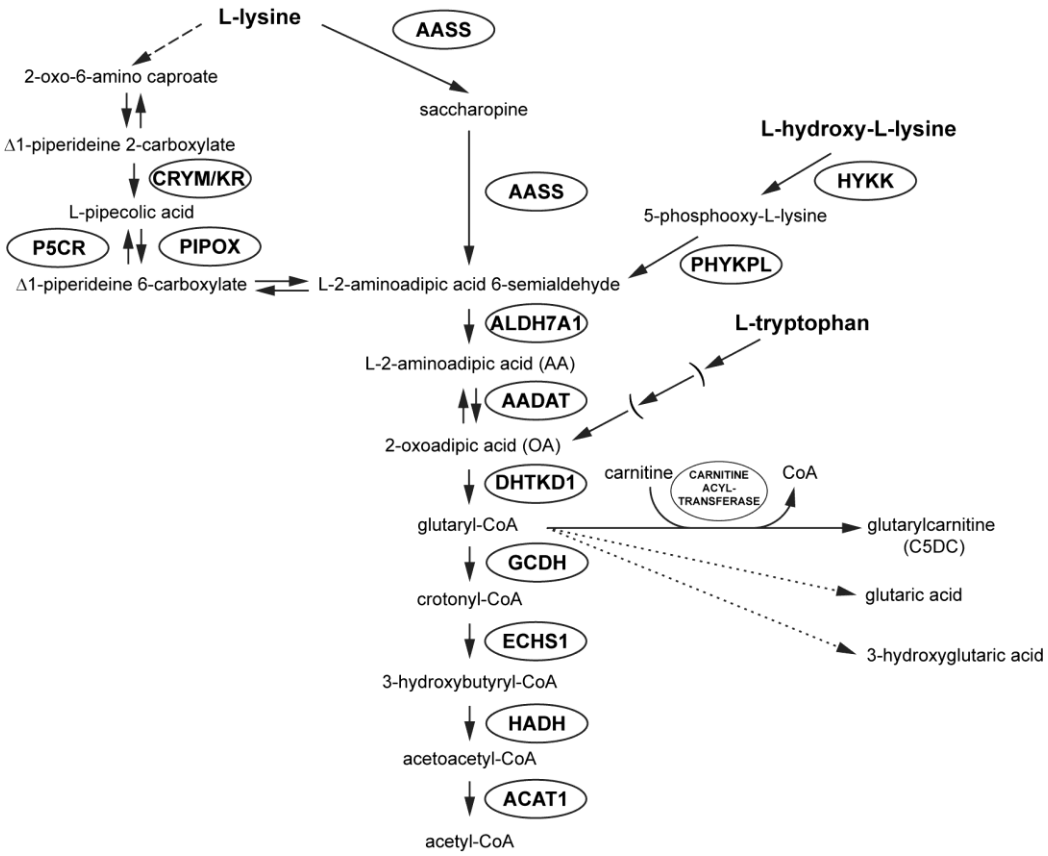

Figure S1. The lysine degradation pathway. (Related to Fig. 1)
The degradation of L-lysine may occur via two pathways: the saccharopine and the pipecolic acid pathway. The mitochondrial saccharopine pathway is well established and is the major pathway. It consists of nine different enzymatic steps that ultimately yield 2 acetyl-CoAs and several reducing equivalents. The pipecolic acid pathway, which is thought to be more active in the brain, proceeds via oxidative deamination with L-pipecolic acid as intermediate. Degradation of L-hydroxy-L-lysine leads to L-2-aminoadipic acid 6-semialdehyde and cytosolic degradation of tryptophan with kynurenine as intermediate leads to the production of OA. The intermediate OA is metabolized into glutaryl-CoA via oxidative decarboxylation by the DHTKD1, the E1 subunit of the 2-oxoadipic acid dehydrogenase complex (OADHc). Glutaryl-CoA is converted into crotonyl-CoA via oxidative decarboxylation by GCDH. The GCDH protein is deficient in GA1 leading to the accumulation of glutaryl-CoA metabolites: glutarylcarnitine (C5DC), glutaric acid and 3-hydroxyglutaric acid. The level of AA correlates with the amount of OA by reversible transamination catalyzed by AADAT. C5DC is the product of detoxification of accumulating glutaryl-CoA through conjugation with carnitine. AASS, alpha-aminoadipic semialdehyde synthase; ALDH7A1, alpha-aminoadipic semialdehyde dehydrogenase; AADAT, kynurenine/alpha-aminoadipate aminotransferase; CRYM/KR, μ-crystallin/ketimine reductase; DHTKD1, dehydrogenase E1 and transketolase domain containing 1; GCDH, glutaryl-CoA dehydrogenase; ECHS1, enoyl-CoA hydratase; HADH, hydroxyacyl-coenzyme A dehydrogenase; ACAT1, acetyl-CoA acetyltransferase; P5CR, pyrroline-5-carboxylate reductase; PIPOX, peroxisomal sarcosine oxidase; HYKK, hydroxylysine kinase; PHYKPL, 5-phosphohydroxy-L-lysine phospho-lyase. Dashed arrows represent not fully characterized enzymatic steps.

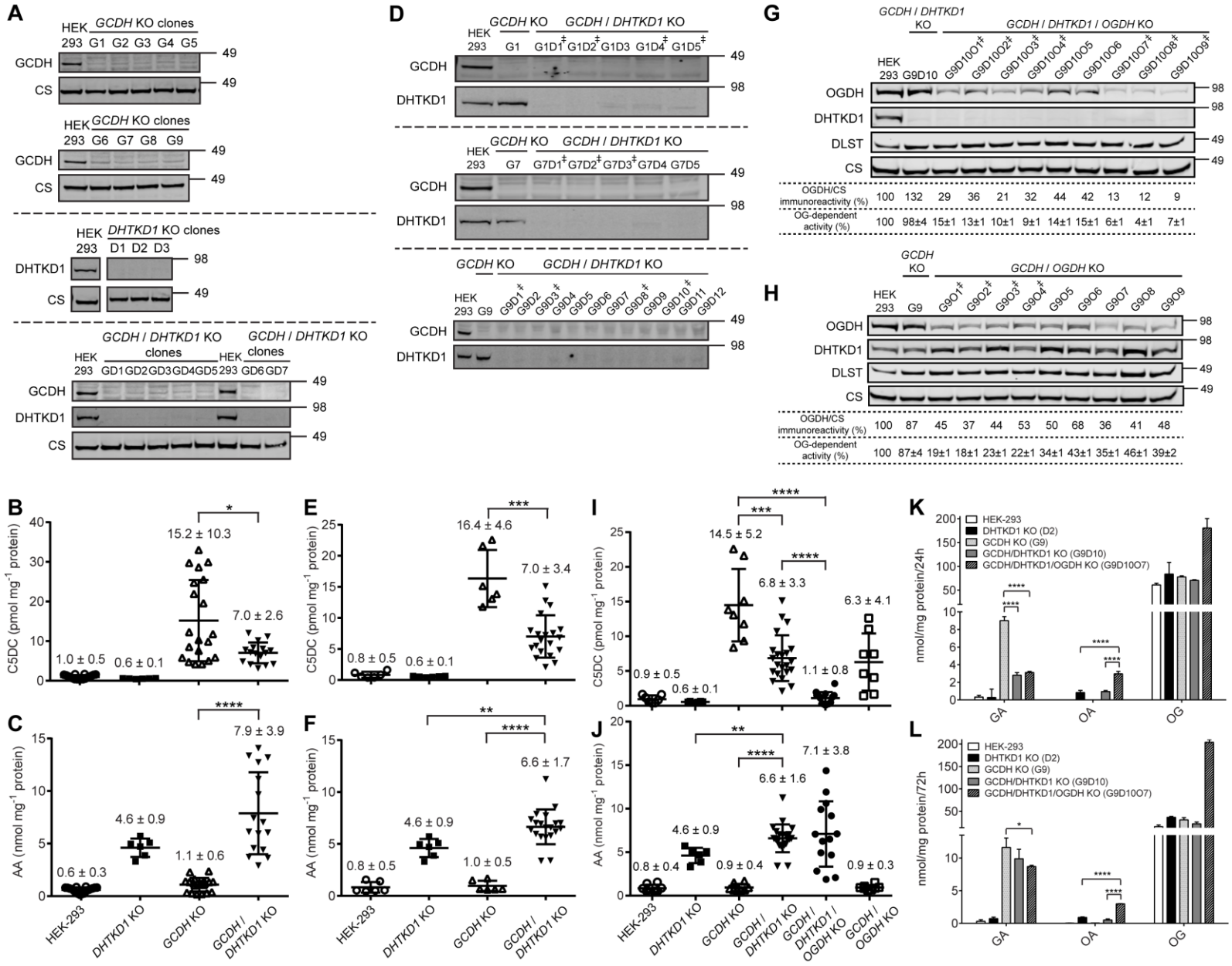
A
HEK 293
GCDH KO clones
G1 G2 G3 G4 G5
G6 G7 G8 G9
DHTKD1 KO clones
D1 D2 D3
GCDH / DHTKD1 KO clones
GD1 GD2 GD3 GD4 GD5 GD6 GD7
GCDH
DHTKD1
CS
49
98
D
GCDH KO
GCDH / DHTKD1 KO
G1D1‡ G1D2‡ G1D3 G1D4‡ G1D5‡
G7D1‡ G7D2‡ G7D3‡ G7D4 G7D5
G9D1‡ G9D2 G9D3‡ G9D4 G9D5 G9D6 G9D7 G9D8‡ G9D9 G9D10‡ G9D11 G9D12
G
GCDH / DHTKD1 KO
GCDH / DHTKD1 / OGDH KO
G9D10O1‡ G9D10O2‡ G9D10O3‡ G9D10O4‡ G9D10O5 G9D10O6 G9D10O7‡ G9D10O8‡ G9D10O9‡
OGDH
DLST
OGDH/CS immunoreactivity (%) 100 132 29 36 21 32 44 42 13 12 9
OG-dependent activity (%) 100 98±4 15±1 13±1 10±1 9±1 14±1 15±1 6±1 4±1 7±1
H
GCDH KO
GCDH / OGDH KO
G9O1‡ G9O2‡ G9O3‡ G9O4‡ G9O5 G9O6 G9O7 G9O8 G9O9
OGDH/CS immunoreactivity (%) 100 87 45 37 44 53 50 68 36 41 48
OG-dependent activity (%) 100 87±4 19±1 18±1 23±1 22±1 34±1 43±1 35±1 46±1 39±2
B
C5DC (pmol mg-1 protein)
1.0 ± 0.5
0.6 ± 0.1
15.2 ± 10.3
7.0 ± 2.6
C
AA (nmol mg-1 protein)
0.6 ± 0.3
4.6 ± 0.9
1.1 ± 0.6
7.9 ± 3.9
HEK-293
DHTKD1 KO
GCDH KO
GCDH / DHTKD1 KO
E
0.8 ± 0.5
0.6 ± 0.1
16.4 ± 4.6
7.0 ± 3.4
F
0.8 ± 0.5
4.6 ± 0.9
1.0 ± 0.5
6.6 ± 1.7
I
0.9 ± 0.5
0.6 ± 0.1
14.5 ± 5.2
6.8 ± 3.3
1.1 ± 0.8
6.3 ± 4.1
J
0.8 ± 0.4
4.6 ± 0.9
0.9 ± 0.4
6.6 ± 1.6
7.1 ± 3.8
0.9 ± 0.3
GCDH / DHTKD1 / OGDH KO
GCDH / OGDH KO
K
HEK-293
DHTKD1 KO (D2)
GCDH KO (G9)
GCDH/DHTKD1 KO (G9D10)
GCDH/DHTKD1/OGDH KO (G9D10O7)
nmol/mg protein/24h
GA
OA
OG
L
nmol/mg protein/72h

Figure S2. *DHTKD1* KO reduces glutarylcarnitine in simultaneously and sequentially generated *GCDH/DHTKD1* double KO HEK-293 cell lines whereas OGDH KO reduces glutarylcarnitine to basal levels in HEK-293 GCDH/DHTKD1/OGDH triple KO cell lines. (Related to Fig. 2)

(A) Immunoblot verification of *GCDH* single KO (*upper panel*), *DHTKD1* single KO (*middle panel*) and simultaneously generated *GCDH/DHTKD1* double KO (*lower panel*) clonal cell lines. Single *GCDH* KO clones are indicated as G#, single *DHTKD1* KO as D# and simultaneous double *GCDH/DHTKD1* KO clones as GD#. Citrate synthase (CS) was used as loading control. The position of molecular mass marker proteins (in kDa) is given.

(B and C) Biochemical analyses of C5DC (B) and AA (C) levels in HEK-293 *GCDH/DHTKD1* simultaneous double KO (▼) compared with HEK-293 *DHTKD1* single KO (■), HEK-293 *GCDH* single KO (△) and wild-type HEK-293 cells (○).

(D) Immunoblot verification of *GCDH/DHTKD1* double KOs generated from G1 (*upper panel*), G7 (*middle panel*) and G9 (*lower panel*). Single *GCDH* KO clones are indicated as G# and consecutively generated double *GCDH/DHTKD1* knockout clones as G#D#. The position of molecular mass marker proteins (in kDa) is given. ‡ indicates selected clones to measure the levels of C5DC and AA.

(E and F) Global statistical analyses of C5DC (E) and AA (F) levels in HEK-293 *GCDH/DHTKD1* double KO (▼) compared with HEK-293 *DHTKD1* single KO (■), HEK-293 *GCDH* single KO (△) and wild-type HEK-293 cells (○).

(G and H) Immunoblot verification of triple *GCDH/DHTKD1/OGDH* KO clones generated from G9D10 (G) and of double *GCDH/OGDH* KO clones generate from G9 (H). Single *GCDH* KO clones are indicated as G#, double *GCDH/DHTKD1* KO clones as G#D#, double *GCDH/OGDH* KO clones as G#O# and triple *GCDH/DHTKD1/OGDH* KO clones as G#D#O#. The position of molecular mass marker proteins (in kDa) is given. ‡ indicates selected clones to measure the levels of C5DC and AA. The immunoreactivity of OGDH was determined and normalized to CS levels for each sample and expressed as a percentage relative to OGDH/CS in HEK-293. The oxidative decarboxylation of OG in cell lysates of HEK-293 KOs was measured to evaluate *OGDH* knockout efficiency and is represented as a percentage relative to wild-type activity in HEK-293 cell lysates.

(I and J) Global statistical analyses of C5DC (I) and AA (J) levels in HEK-293 *GCDH*/*DHTKD1*/*OGDH* triple KO (●) and HEK-293 *GCDH*/*OGDH* double KO (□) compared with HEK-293 *GCDH*/*DHTKD1* double KO (▼), HEK-293 *GCDH* single KO (△), HEK-293 *DHTKD1* single KO (■) and wild-type HEK-293 cells (○).

(K and L) Quantification of glutaric acid (GA), OA and OG accumulation in the cell culture media of one clonal cell line for control, *GCDH* KO, *DHTKD1* KO, *GCDH*/*DHTKD1* double KO and *GCDH*/*DHTKD1*/*OGDH* triple KO at 24 (K) and 72 h (L).

Error bars indicate SD and the mean ± SD of C5DC and AA levels are indicated above each group in panels B-C, E-F and I-J. *, $p<0.05$, **, $p<0.01$; ***, $p<0.001$ and ****, $p<0.0001$.

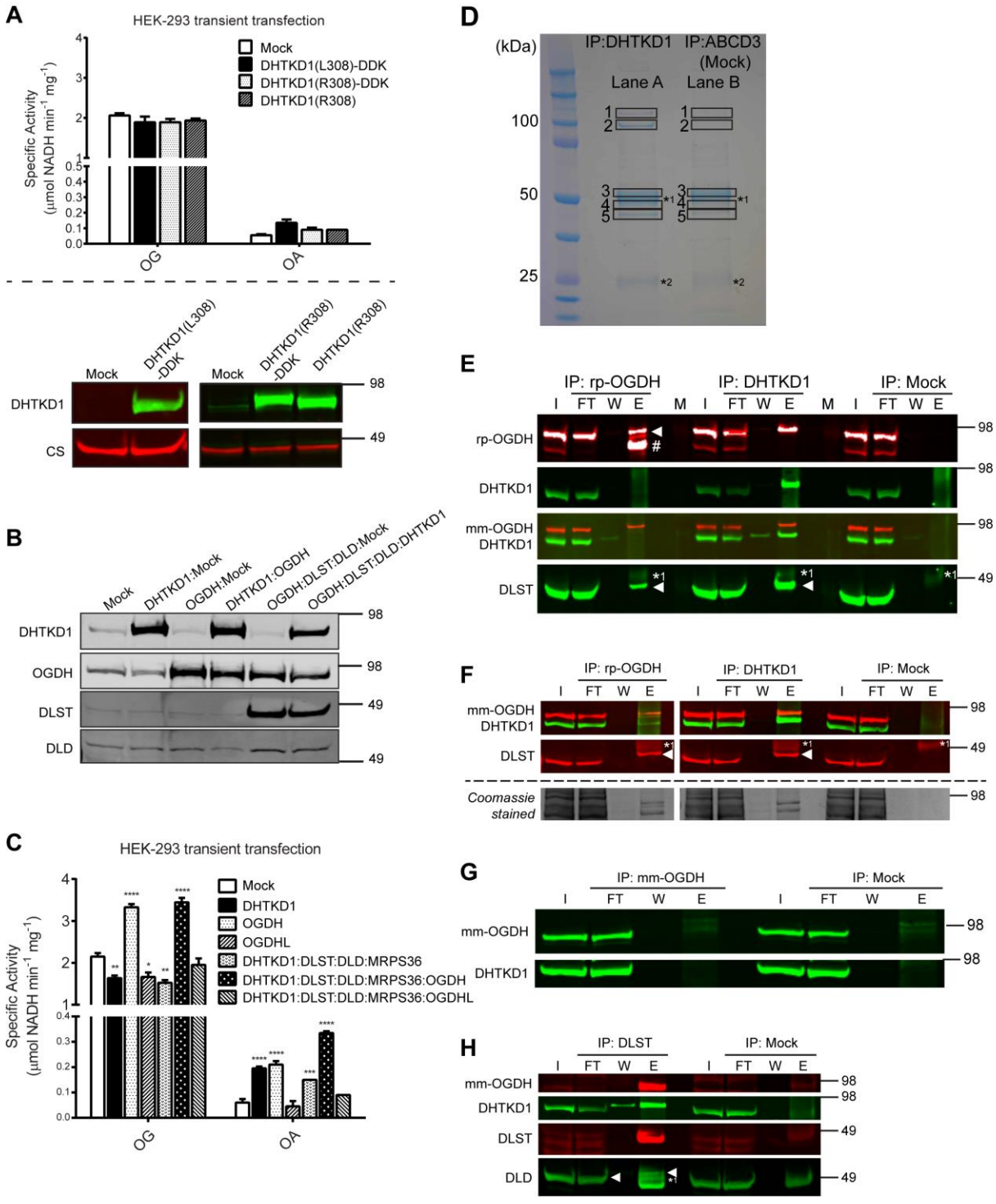
A
HEK-293 transient transfection
Mock
DHTKD1(L308)-DDK
DHTKD1(R308)-DDK
DHTKD1(R308)
Specific Activity (µmol NADH min-1 mg-1)
OG
OA
DHTKD1(L308) -DDK
DHTKD1(R308) -DDK
DHTKD1(R308)
Mock
DHTKD1
CS
98
49
B
Mock
DHTKD1:Mock
OGDH:Mock
DHTKD1:OGDH
OGDH:DLST:DLD:Mock
OGDH:DLST:DLD:DHTKD1
DHTKD1
OGDH
DLST
DLD
98
98
49
49
C
HEK-293 transient transfection
Mock
DHTKD1
OGDH
OGDHL
DHTKD1:DLST:DLD:MRPS36
DHTKD1:DLST:DLD:MRPS36:OGDH
DHTKD1:DLST:DLD:MRPS36:OGDHL
Specific Activity (µmol NADH min-1 mg-1)
OG
OA
D
(kDa)
IP:DHTKD1
IP:ABCD3 (Mock)
Lane A
Lane B
100
50
25
E
IP: rp-OGDH
IP: DHTKD1
IP: Mock
I FT W E M I FT W E M I FT W E
rp-OGDH
DHTKD1
mm-OGDH
DHTKD1
DLST
98
98
98
49
F
IP: rp-OGDH
IP: DHTKD1
IP: Mock
mm-OGDH
DHTKD1
DLST
Coomassie stained
98
49
98
G
IP: mm-OGDH
IP: Mock
mm-OGDH
DHTKD1
98
98
H
IP: DLST
IP: Mock
mm-OGDH
DHTKD1
DLST
DLD
98
98
49
49

Figure S3. Overexpression of DHTKD1 and OGDH increase the oxidative decarboxylation of 2-oxoadipic acid and immunoprecipitation of DHTKD1 with interacting partners from DBA/2J mouse liver or kidney. (Related to Fig. 3).

(A) (*upper panel*) Oxidative decarboxylation of OG and OA in cell lysates of HEK-293 cells upon transient transfection with a rare *DHTKD1* variant (L308), the common variant (R308) and without C-terminal tags. 6.9 μg of each plasmid construct was used for transfection. (lower *panel*) Immunoblot of HEK-293 transient transfections depicted on the upper panel. Citrate synthase (CS) was used as loading control and DDK denotes the C-terminal FLAG tag. The position of molecular mass marker proteins (in kDa) is given.

(B) Immunoblot of HEK-293 transient transfections depicted on Fig. 3A and Fig. S3C. The position of molecular mass marker proteins (in kDa) is given.

(C) Oxidative decarboxylation of OG and OA in cell lysates of HEK-293 cells upon transient transfection of the indicated genes: *DHTKD1*, *DLST*, *DLD*, *OGDH*, *OGDHL* and *MRPS36*. The amount of DNA has been maintained constant as follows: 6.9 μg in Mock, DHTKD1, OGDH and OGDHL conditions; 1.73 μg of each construct in DHTKD1:DLST:DLD:MRPS36 condition; and 1.38 μg of each construct in DHTKD1:DLST:DLD:MRPS36:OGDH and DHTKD1:DLST:DLD:MRPS36:OGDHL conditions.

(D) Coomassie-stained SDS-PAGE gel of DHTKD1 interacting proteins (lane A) and negative control (lane B). Gel pieces (1 through 5) were cut out for mass spectrometry-based protein identification. $*^1$ and $*^2$ indicate the heavy and light chain of the IP antibody, respectively. The position of molecular mass marker proteins (in kDa) is given. Proteins specifically identified in each gel slice are shown in Table S1.

(E) OGDH was immunoprecipitated from liver homogenate of DBA/2J mouse using a rabbit polyclonal anti-OGDH antibody (rp-OGDH, GTX33374). (*upper panel*) The triangle indicates the position of OGDH and # indicates unspecific immunoprecipitation of a protein that was identified as plasminogen by mass spectrometry and is not detected by the monoclonal anti-OGDH antibody. (*lower panel*). The triangle indicates the position of the co-IP protein (DLST) close to the heavy chain of the IP antibody.

(F) OGDH was immunoprecipitated from kidney homogenate of DBA/2J mouse using a rabbit polyclonal anti-OGDH antibody (rp-OGDH, GTX33374). Kidney has a lower expression of plasminogen when compared with liver. Immunoblot analysis showed DLST interacting with OGDH. A band was detected using the anti-DHTKD1 antibody, although with a slightly lower molecular weight than expected for DHTKD1. The triangle indicates the position of the co-IP protein (DLST) close to the heavy chain of the IP antibody.

(G) A third attempt to efficiently immunoprecipitate OGDH from DBA/2J mouse liver homogenate was performed using a monoclonal anti-OGDH antibody (mm-OGDH, 66285-1-lg). No OGDH was detected in the eluted fraction.

(H) DLST was immunoprecipitated from DBA/2J mouse liver homogenate. The triangle indicates the position of the co-IP protein (DLD) close to the heavy chain of the IP antibody. The position of molecular mass marker proteins (in kDa) is given.

Aliquots of homogenate (I, input: 2.5% of total fraction volume), the unbound protein after incubation with IP antibody (FT, flow-through: 2.5% of total fraction volume), the last wash (W: 2% of total fraction volume) and eluted fraction (E: 100% of total fraction volume) were analyzed by WB by successively using a rabbit polyclonal anti-OGDH (GTX33374) or mouse monoclonal anti-OGDH (mm-OGDH, 66285-1-lg), anti-DHTKD1, anti-DLST antibodies or Coomassie stained SDS-PAGE gel (E-G) or by successively using anti-DHTKD1, mouse monoclonal anti-OGDH, anti-DLST and anti-DLD antibodies (H). Heavy (*1) chain of IP antibody is indicated.

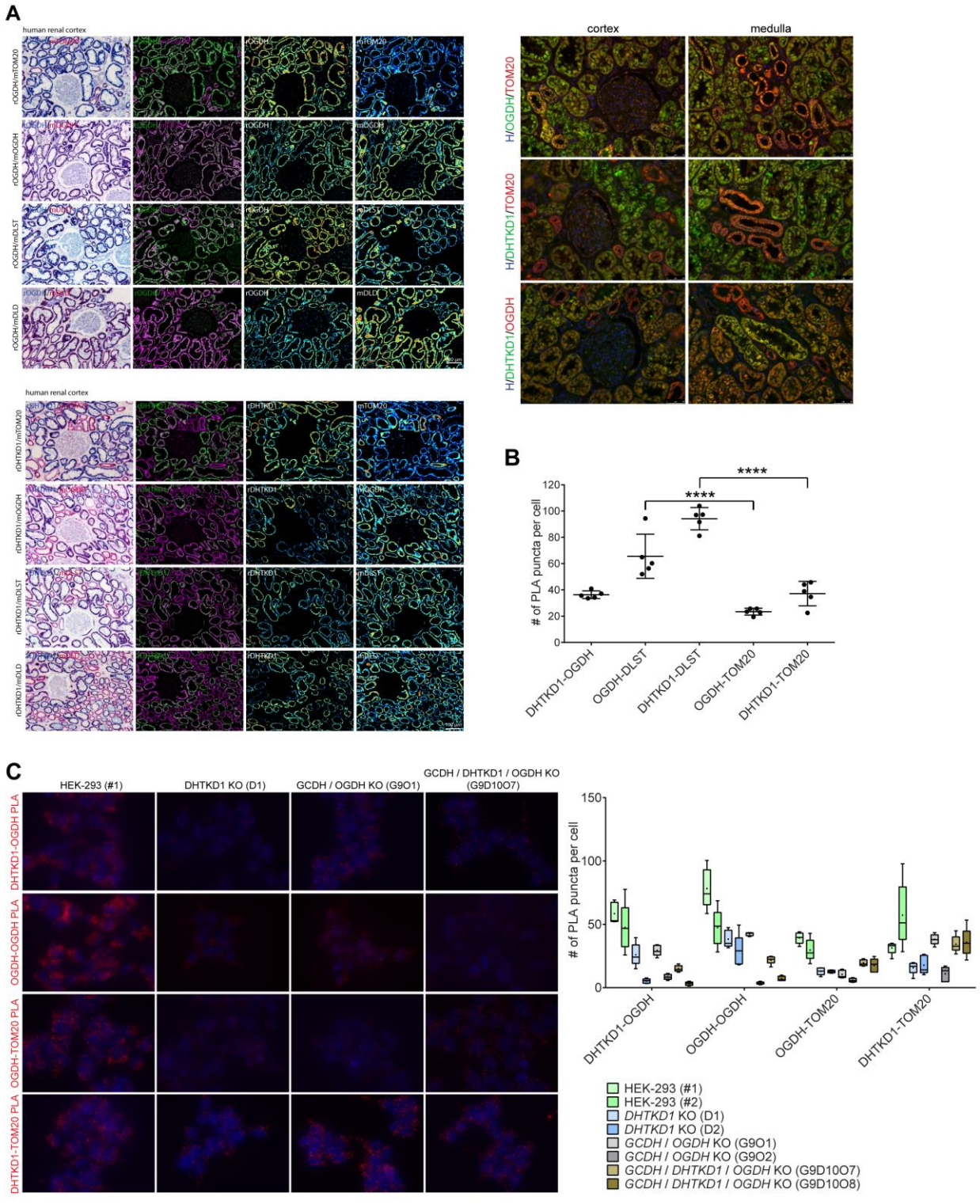
A
human renal cortex
rOGDH/mTOM20
rOGDH/mOGDH
rOGDH/mDLST
rOGDH/mDLD
rOGDH
rTOM20
mOGDH
mDLST
mDLD
human renal cortex
rDHTKD1/mTOM20
rDHTKD1/mOGDH
rDHTKD1/mDLST
rDHTKD1/mDLD
rDHTKD1
mTOM20
mDLST
mDLD
cortex
medulla
H/OGDH/TOM20
H/DHTKD1/TOM20
H/DHTKD1/OGDH
B
# of PLA puncta per cell
****
****
DHTKD1-OGDH
OGDH-DLST
DHTKD1-DLST
OGDH-TOM20
DHTKD1-TOM20
C
HEK-293 (#1)
DHTKD1 KO (D1)
GCDH / OGDH KO (G9O1)
GCDH / DHTKD1 / OGDH KO (G9D10O7)
DHTKD1-OGDH PLA
OGDH-OGDH PLA
OGDH-TOM20 PLA
DHTKD1-TOM20 PLA
# of PLA puncta per cell
DHTKD1-OGDH
OGDH-OGDH
OGDH-TOM20
DHTKD1-TOM20
HEK-293 (#1)
HEK-293 (#2)
DHTKD1 KO (D1)
DHTKD1 KO (D2)
GCDH / OGDH KO (G9O1)
GCDH / OGDH KO (G9O2)
GCDH / DHTKD1 / OGDH KO (G9D10O7)
GCDH / DHTKD1 / OGDH KO (G9D10O8)

Figure S4. Immunofluorescence and proximity ligation assay of DHTKD1 with interacting partners in human kidney and HEK-293 cells, respectively. (Related to Fig. 3).
(A) Colocalization of DHTKD1 and OGDH in human kidney (cortex and medulla cryosections) shown by sequential two-colour brightfield immunostaining (spectral image analysis, left panels) and by double immunofluorescence (right panel). TOM20 was used as a negative control. Scale bars: 100 μm (left panels) and 50 μm (right panel).
(B) Quantification of in situ PLA of OGDH, DHTKD1 and DLST interactions in HEK-293 cells (Fig. 3E). TOM20 was used as a negative control. Error bars indicate SD. ****, $p<0.0001$.
(C) In situ PLA analysis of DHTKD1 and OGDH interaction in HEK-293 and knockout cell lines: *DHTKD1* KO, *GCDH*/*OGDH* KO and *GCDH*/*DHTKD1*/*OGDH* KO. Representative images of PLA (red) from one clone of each cell line and quantification analysis are shown. Clones are identified as in Fig. 2. TOM20 served as a negative control. Scale bars: 10 μm.

Table S1. The genotype distribution in a cross of *Gcdh*$^{+/-}$ *Dhtkd1*$^{D2/B6}$ X *Gcdh*$^{+/-}$ *Dhtkd1*$^{D2/B6}$. Related to Fig. 1.

	Gcdh$^{+/+}$	*Gcdh*$^{+/-}$	*Gcdh*$^{-/-}$
Dhtkd1$^{D2/D2}$	7 (12)	28 (23)	15 (12)
Dhtkd1$^{D2/B6}$	23 (23)	51 (47)	17 (23)
Dhtkd1$^{B6/B6}$	10 (12)	26 (23)	9 (12)

Observed and expected (in parenthesis) progeny. Expected numbers are calculated based on the total number of pups (186). The Chi square statistic for these numbers is 7.054. The threshold for 5 degrees of freedom (# genotypic combinations - # alleles) and an alpha level of 0.05 is 11.0705.

Table S2. Mass spectrometric analysis of interacting proteins identified by IP of DHTKD1 from DBA/2J mouse liver. Related to Fig. 3B.

Gel slice #	Protein Name	Protein accession number	MW[a]	# unique peptides		# exclusive spectra		% sequence coverage	
				Lane A	Lane B	Lane A	Lane B	Lane A	Lane B
1	2-oxoglutarate dehydrogenase	Q60597 (ODO1_MOUSE)	116 kDa (112)	7	0	24	0	7.2	-
	Probable 2-oxoglutarate dehydrogenase E1 component DHKTD1	A2ATU0 (DHTK1_MOUSE)	103 kDa (100)	2	0	3	0	2.0	-
2	2-oxoglutarate dehydrogenase	Q60597 (ODO1_MOUSE)	116 kDa (112)	3	0	3	0	2.5	-
	Probable 2-oxoglutarate dehydrogenase E1 component DHKTD1	A2ATU0 (DHTK1_MOUSE)	103 kDa (100)	17	0	60	0	16.6	-
	Dihydrolipoyllysine-residue succinyltransferase component of 2-oxoglutarate dehydrogenase complex	Q9D2G2 (ODO2_MOUSE)	49 kDa (41)	2	0	2	0	4.6	-
Gel slice #	Protein Name	Protein accession number	MW[a]	# unique peptides		# exclusive spectra		% sequence coverage	
				Lane A	Lane B	Lane A	Lane B	Lane A	Lane B
3	Probable 2-oxoglutarate dehydrogenase E1 component DHKTD1	A2ATU0 (DHTK1_MOUSE)	103 kDa (100)	3	0	3	0	3.1	-
	Dihydrolipoyl dehydrogenase	O08749 (DLDH_MOUSE)	54 kDa (50)	19	3	57	3	39.9	7.5
	Dihydrolipoyllysine-residue succinyltransferase component of 2-oxoglutarate dehydrogenase complex	Q9D2G2 (ODO2_MOUSE)	49 kDa (41)	12	4	43	4	32.8	8.8
4	Probable 2-oxoglutarate dehydrogenase E1 component DHKTD1	A2ATU0 (DHTK1_MOUSE)	103 kDa (100)	3	0	3	0	2.9	-
	Dihydrolipoyl dehydrogenase	O08749 (DLDH_MOUSE)	54 kDa (50)	4	0	4	0	8.3	-
	Dihydrolipoyllysine-residue succinyltransferase component of 2-oxoglutarate dehydrogenase complex	Q9D2G2 (ODO2_MOUSE)	49 kDa (41)	8	0	32	0	17.8	-
5	Probable 2-oxoglutarate dehydrogenase E1 component	A2ATU0 (DHTK1_MOUSE)	103 kDa (100)	1	0	1	0	1.1	-

DHKTD1								
Dihydrolipoyl dehydrogenase	O08749 (DLDH_MOUSE)	54 kDa (50)	2	0	2	0	3.7	-
Dihydrolipoyllysine-residue succinyltransferase component of 2-oxoglutarate dehydrogenase complex	Q9D2G2 (ODO2_MOUSE)	49 kDa (41)	2	0	3	0	4.4	-
Glutaryl-CoA dehydrogenase	Q60759 (GCDH_MOUSE)	49 kDa (44)	1	2	1	2	3.2	5.9

Results represent the proteins specifically identified in each gel slice when peptides were run against a library of proteins likely to interact with DHTKD1 (Protein accession numbers: A2ATU0, Q60597, E9Q7L0, Q9D2G2, O08749, Q60759, Q8BHG1, Q9CQX8 and Q9DCX2. Peptides were selected using a stringent filter (99.0% protein threshold, 1 min. peptide and 95% peptide threshold) to avoid false positives. Sequence coverage represents the percentage of sequence (full length protein) matching with peptides found in the analysis. [a]Molecular weight of processed form of the protein (without mitochondrial transit peptide) is shown in parenthesis.